

CD36 Is Important for Adipocyte Recruitment and Affects Lipolysis

Irene O.C.M. Vroegrijk¹, Jan Bert van Klinken², Janna A. van Diepen¹, Sjoerd A.A. van den Berg², Maria Febbraio³, Laura K.M. Steinbusch^{4*}, Jan F.C. Glatz⁴, Louis M. Havekes^{1,5,6}, Peter J. Voshol^{1*}, Patrick C.N. Rensen¹, Ko Willems van Dijk^{1,2} and Vanessa van Harmelen²

Objective: The scavenger receptor CD36 facilitates the cellular uptake of long-chain fatty acids. As CD36-deficiency attenuates the development of high fat diet (HFD)-induced obesity, the role of CD36-deficiency in preadipocyte recruitment and adipocyte function was set out to characterize.

Design and Methods: Fat cell size and number were determined in gonadal, visceral, and subcutaneous adipose tissue of CD36^{-/-} and WT mice after 6 weeks on HFD. Basal lipolysis and insulin-inhibited lipolysis were investigated in gonadal adipose tissue.

Results: CD36^{-/-} mice showed a reduction in adipocyte size in all fat pads. Gonadal adipose tissue also showed a lower total number of adipocytes because of a lower number of very small adipocytes (diameter <50 μm). This was accompanied by an increased pool of preadipocytes, which suggests that CD36-deficiency reduces the capacity of preadipocytes to become adipocytes. Regarding lipolysis, in adipose tissue from CD36^{-/-} mice, cAMP levels were increased and both basal and 8-bromo-cAMP stimulated lipolysis were higher. However, insulin-mediated inhibition of lipolysis was more potent in CD36^{-/-} mice.

Conclusions: These results indicate that during fat depot expansion, CD36-deficiency negatively affects preadipocyte recruitment and that in mature adipocytes, CD36-deficiency is associated with increased basal lipolysis and insulin responsiveness.

Obesity (2013) **21**, 2037-2045. doi:10.1002/oby.20354

Introduction

Obesity, and in particular abdominal obesity, is associated with several metabolic abnormalities such as insulin resistance and hypertriglyceridemia, which increase the risk of developing type 2 diabetes and eventually cardiovascular morbidity and mortality (1). Obesity is caused by a chronic positive energy balance that increases the storage of triglycerides (TG) in adipose tissue. This storage of energy is partly regulated by fatty acid (FA) transporter proteins in adipocytes, which facilitate the cellular entry of lipoprotein derived FA. One of these FA transporters is CD36 (2,3), an 88 kDa glycoprotein (reviewed in Silverstein and Febbraio [4]) that primarily facilitates the transport of long-chain FA. The role of CD36 in white adipose tissue (WAT) is illustrated by diminished uptake of the FA analogs

BMIPP and IPPA in adipose tissue of CD36-deficient (CD36^{-/-}) mice fed a chow diet (5). Other studies have demonstrated that CD36-deficiency protects against obesity induced by a high fat diet (HFD) (6,7) and development of cardiometabolic problems (8).

Because CD36-deficiency attenuates the development of HFD-induced obesity, we were interested in the role of CD36 in adipocyte development and function. We investigated adipocyte cell size and number in various adipose tissue depots to determine whether CD36-deficiency affects adipocyte hypertrophy (i.e., adipocyte growth) and/or hyperplasia (i.e., recruitment of new adipocytes), as both these parameters determine the expansion capacity of adipose tissue. Moreover, we determined the intracellular lipid accumulation of isolated preadipocytes of CD36^{-/-} versus wild-type (WT) mice *in vitro* after incubation

¹ Department of General Internal Medicine, Endocrinology and Metabolic Diseases, Leiden University Medical Center, Leiden, The Netherlands ² Department of Human Genetics, Leiden University Medical Center, Leiden, The Netherlands. Correspondence: Vanessa van Harmelen (V.J.A.van_Harmelen@lumc.nl)

³ Division Department of Cell Biology, Lerner Research Institute, Cleveland Clinic Foundation, Cleveland, Ohio, USA ⁴ Department of Molecular Genetics, Maastricht University, Maastricht, The Netherlands ⁵ Department of Cardiology, Leiden University Medical Center, Leiden, The Netherlands ⁶ TNO Metabolic Health Research, Gaubius Laboratory, Leiden, The Netherlands

***Present address:** Metabolic Research Laboratories, Institute of Metabolic Science, University of Cambridge, Cambridge, UK. Present address of L.K.M Steinbusch: Center for Integrative Genomics, Université de Lausanne, Lausanne, Switzerland.

Funding Agencies: This work was supported by grants from the Netherlands Organization for Scientific Research (NWO Zon-MW;917.76.301 to P.J.V.) and by grants from the Center of Medical Systems Biology (CMSB), the Netherlands Consortium for Systems Biology (NCSB) established by The Netherlands Genomics Initiative/Netherlands Organization for Scientific Research (NGI/NWO), the Dutch Diabetes Research Foundation (2005.01.003 to P.J.V.), the seventh framework program of the EU-funded "LipidomicNet" (proposal number 202272) and was performed within the framework of CTMM, the Center for Translational Molecular Medicine (www.ctmm.nl), project PREDICt (grant 01C-104), and supported by the Netherlands Heart Foundation, Dutch Diabetes Research Foundation, and Dutch Kidney Foundation. P.C.N.R. is an Established Investigator of the Netherlands Heart Foundation (2009T038).

Disclosure: The authors have no competing interests.

Received: 29 May 2012 **Accepted:** 16 December 2012 **Published online** 20 March 2013. doi:10.1002/oby.20354

in adipogenic media. In addition, lipolysis rate of isolated mature adipocytes of CD36-deficient mice versus WT mice was determined, as adipocyte volume is not only determined by uptake of FA, which lead to TG storage, but also by the level of FA release during the process of adipocyte lipolysis. Taken together, we aimed to investigate the role of CD36 in adipocyte development and function, because CD36 is involved in the development of diet-induced obesity. The current study shows that CD36 affects both adipocyte recruitment and lipolysis.

Methods

Animals

The generation of CD36^{-/-} mice has been described previously (9). For this study, CD36^{-/-} mice were crossed back eight times to the C57Bl/6J background. CD36^{-/-} mice were bred at the Leiden University Medical Center, Leiden, The Netherlands. WT control mice (C57Bl/6J background) were purchased from Charles River (Maasricht, The Netherlands). The mice used in experiments were male, housed under standard conditions with free access to water and food. Mice were fed a HFD (45% energy derived from lard fat; D12451, Research Diet Services, Wijk bij Duurstede, The Netherlands) when they were 12 weeks of age to induce obesity. Body weight was measured regularly. All experiments were approved by the animal ethics committee of Leiden University Medical Center.

Body composition

After 11 weeks of HFD feeding body composition was determined in overnight fasted mice using dual energy X-ray absorptiometry (DEXA) (Norland Stratec Medizintechnik GmbH, Birkenfeld, Germany).

Generation of TG-rich emulsion particles

Very low-density lipoprotein (VLDL)-like TG-rich emulsion particles were prepared and characterized as described previously (10). Lipids (100 mg) at a weight ratio of triolein:egg yolk phosphatidylcholine:lysophosphatidylcholine:cholesteryl oleate:cholesterol of 70:22.7:2.3:3.0:2.0, supplemented with 100 μ Ci of glycerol tri[9,10(n)-³H]oleate (³H]TO) (GE Healthcare, Little Chalfont, UK) were sonicated at 10 μ m output using a Soniprep 150 (MSE Scientific Instruments, Crawley, UK). Density gradient ultracentrifugation was used to obtain 80 nm-sized emulsion particles, which were used for subsequent experiments. TG content of the emulsions was measured using a commercially available enzymatic kit from Roche Molecular Biochemicals (Indianapolis, IN). Emulsions were stored at 4°C under argon and used within 7 days.

In vivo clearance of TG-rich emulsion particles

To study the *in vivo* clearance of the VLDL-like emulsion particles, mice were fed a HFD for 13 weeks. Mice were fasted 4 h (from 8.00 am to 12.00 pm) prior to the start of the experiment and anesthetized by intraperitoneal injection of acepromazine (6.25 mg/kg Neurotranq, Alfasan International BV, Weesp, The Netherlands), midazolam (6.25 mg/kg Dormicum, Roche Diagnostics, Mijdrecht, The Netherlands), and fentanyl (0.31 mg/kg Janssen Pharmaceuticals, Tilburg, The Netherlands). Subsequently, mice were injected ($t = 0$) intravenously with 200 μ L of [³H]TO-labeled emulsion particles at a dose of 1 mg of TG per mouse. Blood samples were taken from the tail at 2, 5, 10, 20, and 30 minutes after injection and plasma ³H-activity was counted. Plasma volumes in milliliter were calculated as $0.04706 \times \text{body weight (g)}$ as determined from ¹²⁵I-BSA clearance studies as described previously (11). After taking the last blood

sample, the liver, heart, spleen, quadriceps, brown adipose tissue, and WAT (i.e., gonadal, visceral, and subcutaneous) were collected. Organs were dissolved overnight at 60°C in Tissue Solubilizer (Amersham Biosciences, Rosendaal, The Netherlands) and ³H-activity was counted. Uptake of [³H]TO-derived radioactivity by the organs was calculated from the ³H activity in each organ divided by plasma-specific activity of [³H]TG and expressed per milligram wet tissue weight. Values were corrected for plasma radioactivity present in the respective tissues (12).

Liver lipids

Lipids were extracted from livers of WT and CD36^{-/-} mice fed a HFD for 11 weeks according to a modified protocol from Bligh and Dyer (13). Briefly, small liver pieces were homogenized in ice-cold methanol. After centrifugation, lipids were extracted by addition of 1800 μ L chloroform:methanol (3:1 v/v) to 45 μ L homogenate. The chloroform phase was dried and dissolved in 2% Triton X-100. Hepatic TG and total cholesterol (TC) concentrations were measured using commercial kits (11488872 and 236691, Roche Molecular Biochemicals, Indianapolis, IN).

Hepatic phospholipid (PL) concentrations were measured using the commercial available kit phospholipids B (Wako Chemicals GmbH, Neuss, Germany). Liver lipids were expressed per mg protein, which was determined using the BCA protein assay kit (Thermo Fisher Scientific, Etten-Leur, The Netherlands).

Determination of adipocyte size, adipocyte lipolysis, and preadipocyte differentiation capacity

To measure adipocyte size, mice were fed a HFD for 6 weeks and killed. Gonadal, visceral, and subcutaneous fat pads were removed and kept in PBS. It was decided to perform the adipocyte morphology and functionality experiments at the week 6 time point to be sure that metabolic adaptations to a HFD were still occurring in the animals and a new set-point had not yet been reached. The tissue was minced and digested in 0.5 g/L collagenase in HEPES buffer (pH 7.4) with 20 g/L of dialyzed bovine serum albumin (BSA, fraction V, Sigma, St Louis, MO, USA) for 1 h at 37°C. The disaggregated adipose tissue was filtered through a nylon mesh with a pore size of 236 μ m. For the isolation of mature adipocytes, cells were obtained from the surface of the filtrate and washed several times. Cell size was determined using an image-processing technique implemented in MATLAB, which automatically determines adipocyte sizes of hundreds of adipocytes from microscopic pictures of isolated adipocytes (~1,000 cells/fat tissue sample). A manuscript describing the method is under preparation. From the measured cells the adipocyte size distribution, mean adipocyte diameter, and adipocyte number per fat pad were determined. Also the volume-weighted mean adipocyte diameter was calculated, which is a measure of the mean adipocyte diameter corrected for the amount of fat that an adipocyte can store (14). In addition, the anti-lipolytic effect of insulin was determined in the adipocytes by incubating them for 2 h at 37°C in DMEM/F12 with 2% BSA in combination with or without 8-bromoadenosine 3'-5'-cyclic monophosphate (8b-cAMP) (10^{-3} M) (Sigma) and/or insulin (10^{-11} M, 10^{-9} M, and 10^{-7} M). Glycerol concentrations (index of lipolysis) were determined using a commercially available free glycerol kit (Sigma) with the inclusion of the hydrogen peroxide-sensitive fluorescence dye Amplex Ultra Red, as described by Clark et al. (15).

For the isolation of preadipocytes, the infranatant of the adipose tissue filtrate was centrifuged at 200g for 10 min at room temperature

and treated with erythrocyte lysis buffer. The cells were washed two times, resuspended in DMEM/NUT.MIX.F12 medium and supplemented with 10% fetal calf serum (FCS) and 100 µg/mL penicillin-streptomycin, and inoculated into 96-well plates (6 wells/adipose tissue region) at a density of 30,000 cells/mL and kept at 37°C, in 5% CO₂. The cells were expanded until confluency after which adipocyte differentiation was induced using an adipogenic medium containing DMEM/F12 with dexamethasone 0.1 µM, 3-isobutyl-1-methylxanthine (IBMX) 25 µM, insulin 17 nM, indomethacin 60 µM, 10% FCS, and 100 µg/mL penicillin-streptomycin. After 4 days, medium was changed to maintenance medium containing insulin 17 nM and 10% FCS. After 1 more day the cells were lipid filled and intracellular lipid accumulation was determined using a fluorometer after incubating the cells with Nile Red (Sigma-Aldrich).

Adipose tissue cyclic AMP level, RNA isolation, and qPCR analysis

Adenosine 3'-5'-cyclic monophosphate (cyclic AMP, cAMP) levels were determined in gonadal fat samples of mice fed a HFD for 6 weeks using the cAMP direct immunoassay kit from Biovision (Biovision, Inc, Milpitas, CA, USA) according to the instructions of the manufacturer. RNA from gonadal fat of mice was isolated using the Nucleospin RNA/Protein kit (Macherey-Nagel, Düren, Germany) according to the instructions of the manufacturer. The quality of each mRNA sample was examined by lab-on-a-chip technology using Experion Stdsens analysis kit (Bio-Rad, Hercules, CA, USA). A total of 600 ng of total RNA was reverse-transcribed with iScript cDNA synthesis kit (Bio-Rad) and obtained cDNA was purified with Nucleospin Extract II kit (Macherey-Nagel). Real-time PCR was carried out on the IQ5 PCR machine (Bio-Rad) using the Sensimix SYBR Green RT-PCR mix (Quantace, London, UK) and QuantiTect SYBR Green RT-PCR mix (Qiagen). mRNA levels were normalized to mRNA levels of glyceraldehyde-3-phosphate dehydrogenase (Gapdh). Primer sequences are listed in Table 1.

Hyperinsulinemic–euglycemic clamp analysis

To assess insulin sensitivity, we fed mice a HFD for 11 weeks. Hyperinsulinemic–euglycemic clamps were performed as described earlier (16). Briefly, after an overnight fast, animals were anesthetized as described above and an infusion needle was placed in the tail vein. Basal glucose

parameters were determined during a 60-min period, by infusion of D-[3-³H]glucose to achieve steady-state levels. A bolus of insulin (3 mU) was given and a hyperinsulinemic–euglycemic clamp was started with a continuous infusion of insulin (5 mU/h) and D-[3-³H]glucose and a variable infusion of 12.5% D-glucose (in PBS) to maintain blood glucose levels at euglycemic levels. Blood samples were taken every 5-10 min from the tip of the tail to monitor plasma glucose levels (Accu-Check). Seventy, eighty, and ninety minutes (steady-state) after the start of the clamp, blood samples (70 µL) were taken for determination of plasma glucose and insulin using commercially available kits (Instruchemie, Delfzijl, the Netherlands and Crystal Chem Inc., Downers Grove, IL). Turnover rates of glucose (µmol/min/kg) were calculated during the basal period and in steady-state clamp conditions as the rate of tracer infusion (dpm/min) divided by the plasma-specific activity of ³H-glucose (dpm/µmol). All metabolic parameters were expressed per kilogram of body weight. The hepatic glucose production (EGP) is calculated from the rate of disappearance (Rd) and glucose infusion rate (GIR) by the following equation: Rd = EGP + GIR. The Rd is measured from Steele's equation in steady state using the tracer infusion rate (Vin) and plasma-specific activity (SA) of ³H-glucose (dpm/µmol) by the following formula: Rd = Vin/SA.

Statistical analysis

Data are presented as means ± SD. Statistical differences were calculated using the nonparametric Mann–Whitney test or two-way ANOVA (SPSS 16, SPSS Inc, Chicago, IL, USA). A *P*-value < 0.05 was regarded statistically significant.

Results

CD36-deficiency reduces HFD-induced obesity

To induce obesity, we fed male CD36^{-/-} and WT mice a HFD containing 45 energy% fat for 12 weeks, and body weight of the mice was followed during the HFD intervention. CD36^{-/-} mice gained less body weight than WT mice (Figure 1A). After 11 weeks, body composition was determined using DEXA analysis. As compared to WT mice, lean body mass was similar, but total body fat was 36% lower in CD36^{-/-} mice (5.8 ± 1.6 vs. 9.0 ± 3.1 g; *P* < 0.05) (Figure 1B). In line with this observation, weights of isolated fat pads were lower in CD36^{-/-} mice (gonadal fat -38%; *P* < 0.01, visceral fat -35%; *P* < 0.01, subcutaneous fat -31%; *P* < 0.05) (Figure 1C). When mice were fed a HFD for 6 weeks, similar differences in phenotype between WT and CD36^{-/-} mice were observed. Fat pad weights of CD36^{-/-} mice were significantly lower after 6 weeks of HFD (gonadal fat -48%; *P* < 0.001, visceral fat -33%; *P* < 0.01, subcutaneous fat -41%; *P* < 0.001), whereas liver weight was significantly higher (data not shown).

CD36-deficiency decreases uptake of TG-rich particle-derived FA by WAT

To confirm that CD36-deficiency affects the tissue-specific uptake of FA that are derived from TG-rich particles, the plasma clearance and organ distribution of [³H]TO-labeled TG-rich VLDL-like emulsion particles was evaluated in HFD-fed CD36^{-/-} mice versus WT mice. CD36-deficiency did not affect the plasma half-life of [³H]TO (*t*_{1/2} = 5.0 ± 1.7 vs. 6.0 ± 1.3 min) (Figure 2A). These results indicate that CD36^{-/-} mice have equal capacity to clear TG-derived FA from plasma. However, tissue distribution of these FA was different for the two mouse strains. CD36-deficiency significantly decreased the uptake

TABLE 1 Primers used for quantitative real-time PCR analysis

Gene	Forward primer	Reverse primer
<i>F4/80</i>	CTTTGGCTATGGGCTTCAGTC	GCAAGGAGGACAGAGTTTATCGTG
<i>MRC-1</i>	GAGAGCCAAGCCATGAGAAC	GTCTGCACCCTCCGGTACTA
<i>MCP-1</i>	GCATCTGCCCTAAGGTCTTCA	TTCACTGTCACACTGGTCACCTCCTA
<i>IL-6</i>	ACCACGGCCTTCCCTACTTC	CTCATTTCCACGATTTCCCAG
<i>IL-10</i>	GACAACATACTGCTAACCAGACTC	ATCACTCTTACCTGCTCCACT
<i>HSL</i>	AGACACCAGCCAACGGATAC	ATCACCCCTCGAAGAAGAGCA
<i>ATGL</i>	ACAGTGTCCCATCTCAGG	TTGGTTCACTAGGCCATTCC
<i>CD45</i>	GTTTTGCTACATGACTGCACA	AGGTTGTCCAACCTGACATCTTTC
<i>CD31</i>	CTGCCAGTCCGAAATGGAAC	CTTCATCCACCGGGGCTATC
<i>GAPDH</i>	TGCACCACCAACTGCTTAGC	GGCATGGACTGTGGTCAATGAG

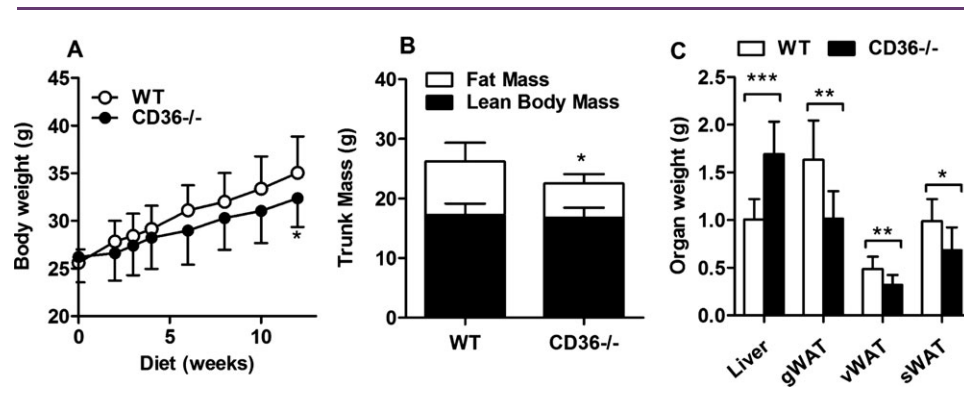


FIGURE 1 CD36-deficiency reduces HFD-induced obesity. In a first set of mice, WT and CD36-deficient (CD36^{-/-}) mice were fed a HFD for 12 weeks. Body weight of WT mice and CD36^{-/-} mice was measured at the indicated time points (A). Values are means \pm SD ($n = 19$ -20 per group); * $P < 0.05$. In a second set of mice, after 11 weeks of HFD and after o/n fast, lean body mass and fat mass were determined using DEXA scan (B). Values are means \pm SD ($n = 7$ -11 per group); * $P < 0.05$. In a third set of mice, after 12 weeks of HFD, tissues were dissected after a 4 h fast and weight of WT tissues and CD36^{-/-} was determined (C). Values are means \pm SD ($n = 10$ per group); * $P < 0.05$, ** $P < 0.01$, *** $P < 0.001$.

of [³H]TO-derived activity in the heart (-38% ; $P < 0.001$), gonadal fat (-29% ; $P < 0.01$), and visceral fat (-30% ; $P < 0.01$), whereas the uptake of [³H]TO-derived activity in the liver ($+42\%$; $P < 0.01$) and spleen ($+49\%$; $P < 0.01$) was significantly increased in the CD36^{-/-} mice (Figure 2B). These results imply that CD36-deficiency increases the flux of FA derived from TG-rich particles toward the liver, while decreasing the flux of FA toward the heart and WAT. Indeed, CD36-deficiency increased hepatic lipid content ($+88\%$; $P < 0.001$) (Figure 2C), without affecting hepatic TC and PL levels (data not shown).

CD36-deficiency decreases adipocyte size in all fat pads and impairs adipocyte recruitment in gWAT

To investigate the effect of reduced FA uptake in adipose tissue on adipocyte morphology, we determined adipocyte size distribution,

volume-weighted mean adipocyte diameter, and total adipocyte number in isolated adipocytes from gonadal, visceral, and subcutaneous fat pads from CD36^{-/-} and WT mice fed a HFD for 6 weeks. In gonadal fat pads of CD36^{-/-} mice, less hypertrophic adipocytes (110 - $170 \mu\text{M}$) were observed (Figure 3A). For visceral and subcutaneous fat, the distribution was also shifted to the left (Figure 3B and C). Volume-weighted mean cell diameter was decreased in gonadal (-12% ; $P < 0.001$), visceral (-14% ; $P < 0.01$), and subcutaneous fat pads (-18% ; $P < 0.001$) of CD36^{-/-} mice, indicating indeed smaller adipocytes (Figure 3D). In gonadal fat, but not in visceral or subcutaneous fat, a decreased number of total adipocytes was observed (-65% ; $P < 0.001$) (Figure 3E).

The number of adipocytes in adipose tissue is dependent upon the recruitment of preadipocytes out of the precursor pool that

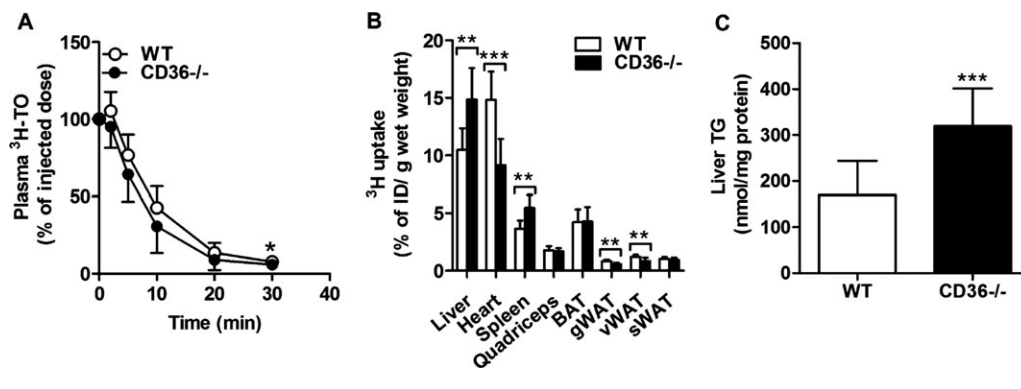


FIGURE 2 CD36-deficiency decreases uptake of TG-rich particle-derived FA by WAT. Wild-type (WT) and CD36-deficient (CD36^{-/-}) mice were fed a HFD for 13 weeks. After a 4 h fast, mice received an intravenous injection of glycerol tri[³H]oleate-labeled VLDL-like emulsion particles (1.0 mg TG). At 2, 5, 10, 20, and 30 minutes after injection; blood samples were taken and ³H activities in plasma were counted and calculated as a percentage of the injected dose (ID) (A). Uptake of radioactivity by various organs of WT and CD36^{-/-} mice was determined and presented as % of injected dose per gram wet weight (B). Values are means \pm SD ($n = 9$); ** $P < 0.01$, *** $P < 0.001$. BAT, Brown adipose tissue; WAT, white adipose tissue; g, gonadal; v, visceral; s, subcutaneous. In a second set of mice, after 12 weeks of HFD, liver TG content was determined and expressed per milligram protein (C). Values are means \pm SD ($n = 10$ -11); *** $P < 0.001$.

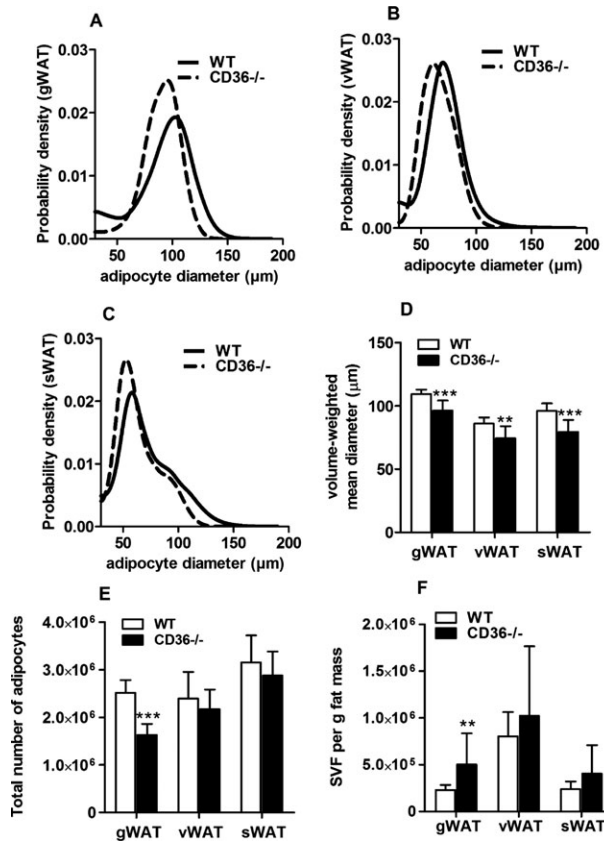


FIGURE 3 CD36-deficiency decreases adipocyte size. WT (solid line) and CD36-deficient (CD36^{-/-}) (dashed line) mice were fed a HFD for 6 weeks. Gonadal (gWAT), visceral (vWAT), and subcutaneous (sWAT) WATs were dissected. Adipocytes were isolated and adipocyte size distribution was determined (A-C). Values are means (n = 9-10). Volume-weighted mean diameter (D) and total number of adipocytes were calculated (E). SVF was obtained and total number of cells in SVF of gWAT, vWAT, and sWAT was determined (F). Values are means ± SD (n = 9-10); **P < 0.01, ***P < 0.001.

differentiate into adipocytes. The total number of cells in the stromal vascular fraction (SVF) (which includes the preadipocyte pool) was higher per gram of gonadal fat in CD36^{-/-} mice ($5.0 \times 10^5 \pm 3.3 \times 10^5$ vs. $2.3 \times 10^5 \pm 5.3 \times 10^4$ cells; $P < 0.01$), indicating that the preadipocyte pool may be larger in gonadal fat of CD36^{-/-} mice. In contrast, for visceral and subcutaneous fat, no differences were observed in number of cells in the SVF (visceral: $1.0 \times 10^6 \pm 7.4 \times 10^5$ vs. $8.0 \times 10^5 \pm 2.6 \times 10^5$ and subcutaneous: $4.0 \times 10^5 \pm 3.0 \times 10^5$ vs. $2.4 \times 10^5 \pm 8.2 \times 10^4$) (Figure 3F).

The SVF is a mixture of cell types where preadipocytes, leukocytes, and endothelial cells constitute the major cell populations. mRNA expression of DLK1, a preadipocyte marker, tended to be higher in gonadal fat pads of CD36^{-/-} mice (CD36^{-/-} mice had a 44% higher DLK-1 expression; $P = 0.09$), whereas expression of CD45, a leukocyte marker, was lower in CD36^{-/-} mice (-39%; $P < 0.01$), and CD31, an endothelial cell marker, was similar for CD36^{-/-} and WT mice (Figure 4A). These data indicate that the increased number of cells in the SVF may be accounted for by an increased number of preadipocytes, but not of leukocytes or endothelial cells. The number of very small adipocytes (diameter <50 µm), on the contrary,

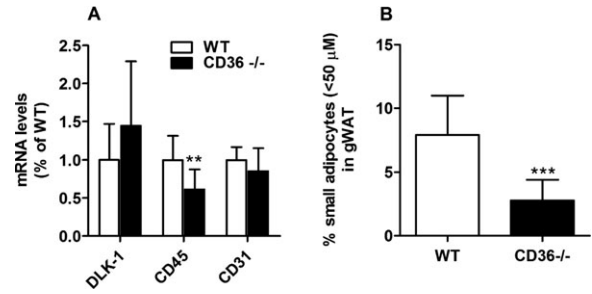


FIGURE 4 CD36-deficiency impairs adipocyte recruitment in gonadal WAT. Wild-type WT and CD36-deficient (CD36^{-/-}) mice were fed a HFD for 6 weeks. Gonadal WAT (gWAT) was dissected and mRNA levels of DLK-1, CD45, and CD31 in gWAT were determined (A). Values are means ± SD (n = 10); **P < 0.01. In addition, the % of very small adipocytes (<50 µm) in gWAT was calculated (B). Values are means ± SD (n = 9-10); ***P < 0.001.

was much lower in the gonadal adipose tissue of CD36^{-/-} mice (-65%; $P < 0.001$) (Figure 4B), which may indicate that less adipocytes are being recruited within gonadal fat pads of CD36^{-/-} mice on a HFD, resulting in a higher pool of preadipocytes that remains in their SVF. This is illustrated in Figure 3A by the bimodal cell size distribution in the gonadal fat of WT mice as opposed to the single peak in the cell size distribution in CD36^{-/-} mice.

CD36-deficiency does not affect preadipocyte intracellular lipid accumulation

To further study the underlying mechanisms that may explain the morphology of adipocytes in CD36^{-/-} mice, we determined the intracellular lipid accumulation in these cells. This was assessed using isolated preadipocytes from CD36^{-/-} and WT mice that were differentiated in an adipogenic medium. No differences were observed in intracellular lipid accumulation between CD36^{-/-} and WT mice for all fat pad regions (Figure 5).

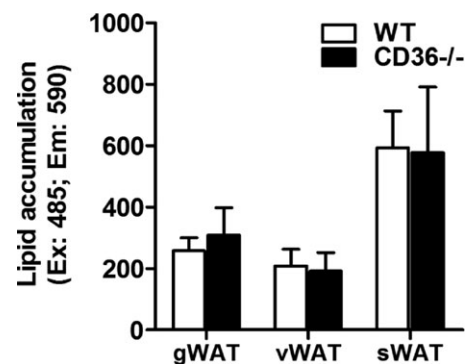


FIGURE 5 CD36-deficiency does not affect preadipocyte intracellular lipid accumulation. Wild-type (WT) and CD36-deficient (CD36^{-/-}) mice were fed a HFD for 6 weeks. Gonadal (gWAT), visceral (vWAT), and subcutaneous (sWAT) WATs were dissected and preadipocytes were isolated and differentiated in adipogenic medium. Lipid accumulation was determined with Nile Red. Values are means ± SD (n = 9-10) (six wells/adipose tissue region per mouse).

CD36-deficiency stimulates lipolysis but improves insulin-mediated inhibition of lipolysis

Morphology of adipocytes is not only determined by uptake of FA, which leads to TG storage, but also by the level of FA release because of lipolysis. To investigate whether CD36 plays a role in lipolysis, we determined basal lipolysis in isolated mature gonadal adipocytes of CD36^{-/-} versus WT mice. Only gonadal adipocytes were studied because only from the gonadal fat pad the yield of adipocytes was enough to perform these experiments. CD36^{-/-} mice had higher glycerol release both expressed per gram adipose tissue (data not shown) and expressed as lipolysis per adipocyte, which was found for both unstimulated and 8-bromo-cAMP (8b-cAMP) stimulated cells (2.1-fold and 2.8-fold, respectively; $P < 0.05$) (Figure 6A). To test whether the increased lipolysis was because of higher levels of the lipolytic enzymes adipose triglyceride lipase (ATGL) and hormone sensitive lipase (HSL), we determined mRNA expression of these enzymes. However, both ATGL and HSL mRNA were lower in gonadal adipose tissue of CD36^{-/-} versus WT mice (-27% ; $P < 0.01$ and -48% ; $P < 0.001$, respectively) (Figure 6B). On the contrary, cAMP levels, which are reported to stimulate lipolysis, were increased in gonadal fat samples of CD36^{-/-} mice ($+31\%$; $P < 0.05$) (Figure 6C). Also the suppression of lipolysis by insulin was investigated in CD36^{-/-} versus WT mice. Inhibition of lipolysis by three different insulin concentrations (10^{-11} , 10^{-9} , and 10^{-7} M) expressed as % of 8b-cAMP-induced lipolysis was tested. An insulin concentration of 10^{-11} M already maximally suppressed lipolysis, because no further inhibition was found with insulin concentrations of 10^{-9} and 10^{-7} M (two-way ANOVA $F = 0.37$; $P = 0.7$). However, inhibition of lipolysis was more potent in CD36^{-/-} mice compared with WT mice (50% vs. 29%; 2 way ANOVA $F = 10.65$; $P < 0.01$) (Figure 6D). To investigate whether the increased adipocyte insulin sensitivity in lipolysis may be related to changes in adipose tissue inflammation, we determined the expression of inflammatory markers in gonadal adipose tissue. As mentioned above, expression of CD45 was lower in CD36^{-/-} mice. Moreover, a decreased expression of macrophage marker F4/80 (-29% ; $P < 0.05$) and a trend for higher IL-10 expression in gonadal adipose tissue of CD36^{-/-} mice ($+53\%$; $P = 0.08$) (Figure 6E) was observed.

CD36-deficiency decreases hepatic insulin sensitivity

To investigate the effect of decreased adiposity and increased hepatic lipid content on metabolic abnormalities such as insulin resistance, we performed a hyperinsulinemic-euglycemic clamp after an o/n fast. Glucose (5.4 ± 0.7 vs. 5.4 ± 0.7 and 5.8 ± 0.6 vs. 5.6 ± 0.6 mM) and insulin levels (0.5 ± 0.2 vs. 0.4 ± 0.2 and 4.0 ± 0.9 vs. 4.5 ± 1.0 ng/mL) were equal for the two genotypes under basal as well as under hyperinsulinemic conditions. To maintain euglycemia during the insulin infusion, a similar amount of glucose was needed to be infused in CD36^{-/-} mice compared with WT mice (GIR 25.7 ± 12.9 vs. 28.1 ± 5.9 $\mu\text{mol}/\text{min}/\text{kg}$) (Figure 7A). The glucose disposal rates under basal conditions were higher for CD36^{-/-} animals (32.3 ± 8.8 vs. 25.1 ± 4.3 $\mu\text{mol}/\text{min}/\text{kg}$; $P < 0.05$). During hyperinsulinemic conditions, glucose disposal rates were similar for CD36^{-/-} and WT animals (55.2 ± 19.9 vs. 43.7 ± 4.6 $\mu\text{mol}/\text{min}/\text{kg}$), indicating that there was no difference in peripheral insulin sensitivity between CD36^{-/-} mice compared with WT mice (Figure 7B). Nevertheless, the CD36^{-/-} mice developed aggravated hepatic insulin resistance compared with WT mice as indi-

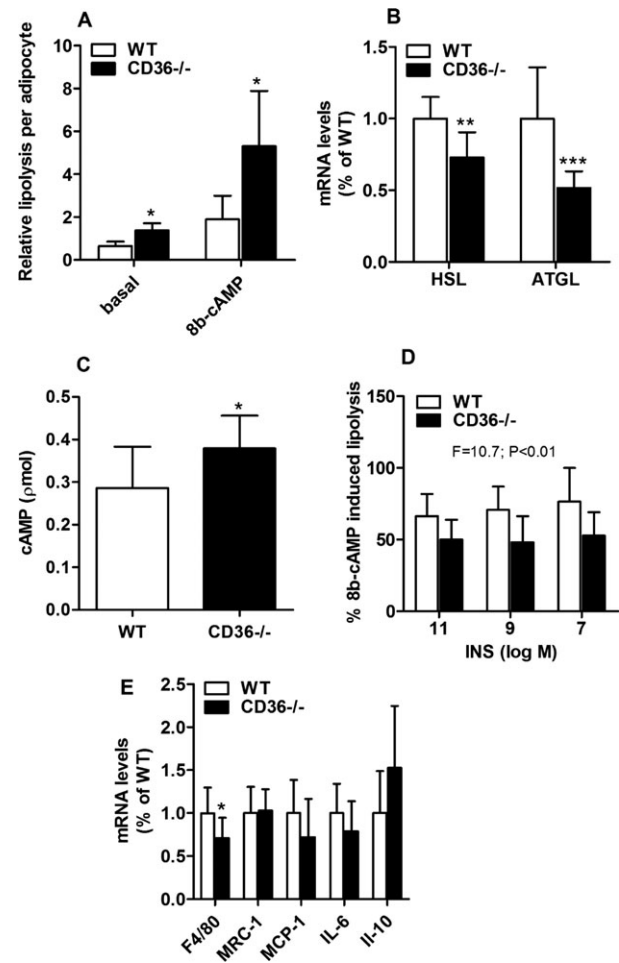


FIGURE 6 CD36-deficiency stimulates lipolysis but improves insulin-mediated inhibition of lipolysis. WT and CD36-deficient (CD36^{-/-}) mice were fed a HFD for 6 weeks. Gonadal (gWAT) was dissected and adipocytes were isolated. Adipocytes were incubated for 2 h at 37°C in DMEM/F12 with 2% BSA in combination with or without 8-bromo-cAMP (8b-cAMP) (10^{-3} M). Glycerol concentrations (index of lipolysis) were determined using a fluorometric method (A). Values are means \pm SD ($n = 5$); $*P < 0.05$. RNA was isolated from gWAT and mRNA levels of ATGL and HSL were determined (B). Values are means \pm SD ($n = 10$); $**P < 0.01$, $***P < 0.001$. gWAT cAMP levels were determined using an immunoassay kit (C). Values are means \pm SD ($n = 9-10$); $*P < 0.05$. The anti-lipolytic effect of insulin was determined as % of 8b-cAMP-induced lipolysis. Adipocytes were incubated with insulin (10^{-11} , 10^{-9} , and 10^{-7} M). Statistical analysis was done using two-way ANOVA (D). Values are means \pm SD ($n = 5$). mRNA levels of macrophage marker F4/80, mannose receptor C1 (MRC-1), monocyte chemoattractant protein-1 (MCP-1), interleukin-6 (IL-6), and IL-10 were determined (E). Values are \pm SD ($n = 10$); $*P < 0.05$.

cated by the higher EGP during hyperinsulinemia (29.3 ± 11.3 vs. 15.5 ± 3.6 $\mu\text{mol}/\text{min}/\text{kg}$; $P < 0.01$) (Figure 7C).

Discussion

The current study investigated the effects of CD36-deficiency on adipocyte morphology and functionality during HFD to get a better understanding of the role of CD36 in adipocytes.

In accordance with others (6,7), we found less adiposity in CD36^{-/-} mice, which was because of a reduced uptake of FA in the adipose

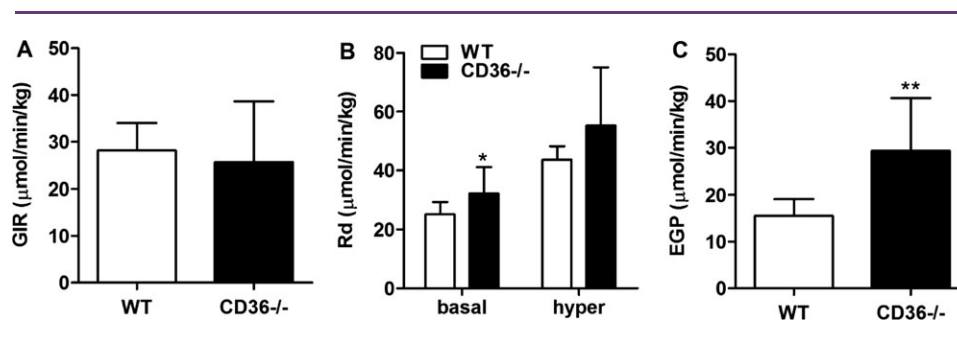


FIGURE 7 CD36-deficiency decreases hepatic insulin sensitivity. WT and CD36-deficient (CD36^{-/-}) mice were fed a HFD for 11 weeks. After o/n fast a hyperinsulinemic-euglycemic clamp was performed. GIR (A), rate of disappearance during basal and hyperinsulinemic period (B) and EGP during hyperinsulinemic period (C) were determined. Values are means ± SD (*n* = 7-10 per group); **P* < 0.05, ***P* < 0.01.

tissues. A decrease in fat pad mass can be caused by smaller adipocytes and/or by a decreased number of adipocytes. The CD36^{-/-} mice showed less hypertrophy of their gonadal, visceral, and subcutaneous adipocytes and the volume-weighted mean cell diameters of all fat pads studied were significantly lower in the CD36^{-/-} mice. Thus, the smaller fat pads in the CD36^{-/-} are because of smaller fat cells in their adipose tissues. Moreover, for the gonadal adipose tissue, the CD36^{-/-} mice showed a lower total number of adipocytes. The gonadal (but neither visceral nor subcutaneous) adipose tissue of CD36^{-/-} mice had a larger pool of preadipocytes, and a reduced number of very small adipocytes (<50 µm). These results suggest that less preadipocytes are being recruited to become adipocytes in the gonadal adipose tissue, resulting in a higher pool of preadipocytes that remain in the SVF. So, the CD36^{-/-} mice seem to have a reduced adiposity not only because of a reduced hypertrophy but also because of a reduced hyperplasia of the adipocytes, at least in the gonadal adipose tissue.

The fact that the observed differences in preadipocyte recruitment seemed restricted to the gonadal tissue may be explained by the gonadal adipose tissue being the largest fat pad in the animals and that it has the largest fat cells, as also shown in this article. We hypothesize that the gonadal adipose tissue was thus exposed to the highest metabolic stress, and therefore, the need for preadipocyte recruitment was probably the highest in this adipose tissue region. There were no differences in gene expression of CD36 between the subcutaneous and gonadal fat pads of WT mice (data not shown), so differential expression of CD36 cannot explain the observation that the gonadal fat is more affected. Gonadal fat depots are larger in male mice, in both absolute and relative terms. In male mice, gonadal fat depots are larger than subcutaneous fat depots after HFD feeding, whereas in female mice, the two fat depots are of almost equal size (17). The current study investigated only male mice, because male mice are more susceptible to diet-induced obesity and diet-induced insulin resistance than female mice (18). It remains to be studied whether in female mice changes in adipose tissue because of CD36-deficiency are less restricted to gonadal adipose tissue.

Interestingly, despite the *in vivo* differences in adipocyte size distributions, isolated preadipocytes showed equal intracellular lipid accumulation *in vitro* for CD36^{-/-} mice and WT for all fat depots. Our results are in line with a recent study from Cai et al. (19) that also showed similar differentiation capacity of the SVF of adipose tissue

between WT and CD36^{-/-} mice. These *in vitro* observations may be explained by *de novo* lipogenesis from carbohydrates present in the culture medium. Collins et al. have shown that *de novo* lipogenesis in differentiating adipocytes can provide all the FA that are necessary for adipocyte maturation. They showed this using an *in vitro* model of human preadipocytes, which are cultured under serum-free conditions without any exogenous fat (20). We added 10% FCS to our mouse preadipocyte cultures—as these cells cannot survive under serum-free conditions and serum contains FA. Despite the availability of exogenous FA as an energy source in our *in vitro* experiments, uptake of FA may have been bypassed and glucose was used instead to synthesize FA intracellularly. The fact that the gonadal adipose tissue of CD36^{-/-} mice showed a reduced preadipocyte recruitment in the *in vivo* experiments may have been due to the HFD, which puts a maximum pressure on the expandability of the adipose tissue. The WT mice were able to cope with the FA overload by delivering them to the existing mature adipocytes as well as to the preadipocytes, whereas in the CD36-deficient mice neither mature adipocytes nor preadipocytes could efficiently take up the excess of FA. During the preparation of this manuscript, a study was published by Christiaens et al. (21) that showed impaired adipogenesis of 3T3-F442A preadipocytes upon CD36 silencing during preadipocyte differentiation. Whether the discrepancies between the studies are because of differences in cell type and/or CD36 expression level (none in our CD36^{-/-} cells, low in the knock-down 3T3-F442A cell line) remains to be determined.

Gonadal adipocytes of CD36^{-/-} mice showed increased basal and 8b-cAMP-induced lipolysis. Published literature suggests that large adipocytes have a higher rate of lipolysis (22). However, we observed a higher basal- and 8b-cAMP-stimulated lipolysis in adipocytes from CD36^{-/-} mice, despite the decreased volume of these adipocytes. The increased lipolysis might be explained by diminished product inhibition of HSL by FA. Because CD36-deficiency impairs FA uptake by adipocytes, less FA might be present intracellularly, which may lead to decreased product inhibition of HSL. Recently, it has been shown that long-chain FA reduce production of cAMP, which results in a decreased phosphorylation of HSL (23). Moreover, it has been shown that A-FABP null mice have decreased lipolysis, whereas E-FABP transgenic mice have increased lipolysis (24). This was explained by FABP being able to bind FA, thereby relieving product inhibition of HSL. We found an unexpected decrease in mRNA levels of ATGL and HSL in adipose

tissue of CD36^{-/-} mice compared to expression in WT mice. However, cAMP levels were increased in CD36^{-/-} mice, which results in increased phosphorylation of HSL rather than increased expression and thus may explain the increased lipolysis. Because muscle normally relies on FA, it might also be that in CD36^{-/-} mice there is a continuous signal from muscle to fat to release more FA and/or that there is absence of a stop signal to inhibit adipocyte lipolysis. Our results are in contrast with Zhou et al. who reported similar basal lipolysis and phosphorylation of HSL by WT and CD36^{-/-} adipose tissue. This discrepancy could be because Zhou et al. (25) measured rates in incubated tissue versus adipocytes in the present study.

Insulin was more potent in inhibiting lipolysis in the CD36-deficient mice, suggesting higher insulin sensitivity of the adipocytes. Hypertrophic subcutaneous adipocytes were associated with increased insulin resistance (26-28). The fact that CD36^{-/-} mice have less hypertrophic adipocytes could therefore help to explain the more potent inhibition of lipolysis by insulin. Kennedy et al. (29) also observed increased insulin sensitivity in adipocytes from CD36^{-/-} mice. They discovered that adipose tissue of HFD-fed CD36^{-/-} mice is less inflamed, which could explain the increased insulin sensitivity. In accordance with these findings, we measured a decreased expression of the leukocyte marker CD45 as well as the macrophage marker F4/80 and found a trend toward higher expression of the antiinflammatory cytokine IL-10 in gonadal adipose tissue of the CD36-deficient mice.

The observed reduction in body weight of CD36^{-/-} mice on HFD is in accordance with recent studies by others, although the effect was less pronounced in our study (-6% vs. -23% and -51%, respectively) (6,7). The smaller effect on body weight gain could be because of differences in HFD composition. We used a HFD containing 45 energy% of fat, whereas others used a HFD containing 60 energy% of fat (6,7).

The reduced FA uptake in adipose tissue in CD36-deficient mice was paralleled by a reduced uptake in heart and an increased FA uptake in the liver and spleen. In contrast to the heart and muscle, CD36 is not a major facilitator of FA uptake in the liver; therefore, FA uptake was not affected by the loss of CD36. Instead, the impaired uptake of FA in other peripheral organs such as muscle and adipose tissue results in a higher flux of FA to the liver. Our findings are partly in accordance with the study of Coburn et al., which showed that uptake of FA analogs was decreased in muscle and adipose tissue of chow-fed CD36^{-/-} mice. We also found that the decreased FA uptake is solely caused by a lack of the FA transporter CD36 and not because of reduced capacity of lipoprotein lipase (LPL), because we found an even higher post-heparin LPL activity in CD36^{-/-} mice (data not shown), probably because of compensatory mechanisms.

The livers of the CD36-deficient mice contained more TG and were more insulin resistant as indicated by the higher EGP under hyperinsulinemic conditions. It is well established that ectopic fat deposition in the liver contributes to development of hepatic insulin resistance (30,31). Although the adipocytes of the CD36^{-/-} mice showed increased insulin sensitivity *in vitro*; *in vivo*, we did not observe increased peripheral insulin sensitivity. This could be because glucose uptake in adipose tissue under hyperinsulinemic conditions is relatively small. Under these conditions, most of the glucose is taken up by heart and muscle (32).

One hypothesis to explain FA trafficking toward other places than adipose tissue, is the so-called “sick adipose tissue” hypothesis (33). According to this hypothesis, unhealthy adipose tissue consists of hypertrophic cells because of impaired creation of new adipocytes. Ultimately, these hypertrophic adipocytes become dysfunctional, which results in increased FA release leading to increased FA availability to nonadipose tissues. Our study shows that CD36-deficiency also leads to “sick adipose tissue.” However, in this case the adipose tissue has dysfunctional adipocytes, which cannot store an overload of FA together with an impaired ability to recruit new adipocytes. As a consequence, the FA are translocated to the liver. Despite the lack of hypertrophic adipocytes, CD36-deficient adipose tissue has an unexpected higher FA release during basal lipolysis, which even further increases the availability of FA to the liver. Therefore, it appears that CD36 plays an important role in adipose tissue functionality—both by regulating FA uptake and release—and likewise the distribution of fat to adipose and nonadipose tissues. **O**

Acknowledgments

The authors thank A.C.M. Pronk and F. el Bouazzaoui for excellent technical assistance.

© 2013 The Obesity Society

References

- Defronzo RA. Insulin resistance, lipotoxicity, type 2 diabetes and atherosclerosis: the missing links. The Claude Bernard Lecture 2009. *Diabetologia* 2010;53(7):1270-1287.
- Abumrad N, Coburn C, Ibrahim A. Membrane proteins implicated in long-chain fatty acid uptake by mammalian cells: CD36, FATP and FABPm. *Biochim Biophys Acta* 1999;1441(1):4-13.
- Abumrad NA, el-Maghrabi MR, Amri EZ, Lopez E, Grimaldi PA. Cloning of a rat adipocyte membrane protein implicated in binding or transport of long-chain fatty acids that is induced during preadipocyte differentiation. Homology with human CD36. *J Biol Chem* 1993;268(24):17665-17668.
- Silverstein RL, Febbraio M. CD36, a scavenger receptor involved in immunity, metabolism, angiogenesis, and behavior. *Sci Signal* 2009;2(72):re3.
- Coburn CT, Knapp FF, Jr., Febbraio M, Beets AL, Silverstein RL, Abumrad NA. Defective uptake and utilization of long chain fatty acids in muscle and adipose tissues of CD36 knockout mice. *J Biol Chem* 2000;275(42):32523-32529.
- Hajri T, Hall AM, Jensen DR, et al. CD36-facilitated fatty acid uptake inhibits leptin production and signaling in adipose tissue. *Diabetes* 2007;56(7):1872-1880.
- Koonen DP, Sung MM, Kao CK, et al. Alterations in skeletal muscle fatty acid handling predisposes middle-aged mice to diet-induced insulin resistance. *Diabetes* 2010;59(6):1366-1375.
- Steinbusch LK, Luiken JJ, Vlasblom R, et al. Absence of fatty acid transporter CD36 protects against Western-type diet-related cardiac dysfunction following pressure overload in mice. *Am J Physiol Endocrinol Metab.* 2011;301(4):E618-E627.
- Febbraio M, Abumrad NA, Hajjar DP, et al. A null mutation in murine CD36 reveals an important role in fatty acid and lipoprotein metabolism. *J Biol Chem* 1999;274(27):19055-19062.
- Rensen PC, Van Berkel TJ. Apolipoprotein E effectively inhibits lipoprotein lipase-mediated lipolysis of chylomicron-like triglyceride-rich lipid emulsions *in vitro* and *in vivo*. *J Biol Chem* 1996;271(25):14791-14799.
- Jong MC, Rensen PC, Dahlmans VE, van der Boom H, Van Berkel TJ, Havekes LM. Apolipoprotein C-III deficiency accelerates triglyceride hydrolysis by lipoprotein lipase in wild-type and apoE knockout mice. *J Lipid Res* 2001;42(10):1578-1585.
- Rensen PC, Herijgers N, Netscher MH, Meskers SC, van EM, Van Berkel TJ. Particle size determines the specificity of apolipoprotein E-containing triglyceride-rich emulsions for the LDL receptor versus hepatic remnant receptor *in vivo*. *J Lipid Res* 1997;38(6):1070-1084.
- Bligh EG, Dyer WJ. A rapid method of total lipid extraction and purification. *Can J Biochem Physiol* 1959;37(8):911-917.
- Jo J, Gavrilova O, Pack S, et al. Hypertrophy and/or hyperplasia: dynamics of adipose tissue growth. *PLoS Comput Biol* 2009;5(3):e1000324.
- Clark AM, Sousa KM, Jennings C, MacDougald OA, Kennedy RT. Continuous-flow enzyme assay on a microfluidic chip for monitoring glycerol secretion from cultured adipocytes. *Anal Chem* 2009;81(6):2350-2356.

16. Voshol PJ, Jong MC, Dahlmans VE, et al. In muscle-specific lipoprotein lipase-overexpressing mice, muscle triglyceride content is increased without inhibition of insulin-stimulated whole-body and muscle-specific glucose uptake. *Diabetes* 2001; 50(11):2585-2590.
17. Macotela Y, Boucher J, Tran TT, Kahn CR. Sex and depot differences in adipocyte insulin sensitivity and glucose metabolism. *Diabetes* 2009;58(4):803-812.
18. Stubbins RE, Najjar K, Holcomb VB, Hong J, Nunez NP. Oestrogen alters adipocyte biology and protects female mice from adipocyte inflammation and insulin resistance. *Diabetes Obes Metab* 2012;14(1):58-66.
19. Cai L, Wang Z, Ji A, Meyer JM, van der Westhuyzen DR. Scavenger receptor CD36 expression contributes to adipose tissue inflammation and cell death in diet-induced obesity. *PLoS One* 2012;7(5):e36785.
20. Collins JM, Neville MJ, Pinnick KE, et al. De novo lipogenesis in the differentiating human adipocyte can provide all fatty acids necessary for maturation. *J Lipid Res* 2011;52(9):1683-1692.
21. Christiaens V, Van Hul M, Lijnen HR, Scroyen I. CD36 promotes adipocyte differentiation and adipogenesis. *Biochim Biophys Acta* 2012;1820:949-956.
22. Laurencikiene J, Skurk T, Kulyte A, et al. Regulation of lipolysis in small and large fat cells of the same subject. *J Clin Endocrinol Metab* 2011;96(12):E2045-E2049.
23. Kalderon B, Azazmeh N, Azulay N, Vissler N, Valitsky M, Bar-Tana J. Suppression of adipose lipolysis by long-chain fatty Acid analogs. *J Lipid Res* 2012;53: 868-878.
24. Hertzel AV, Smith LA, Berg AH et al. Lipid metabolism and adipokine levels in fatty acid-binding protein null and transgenic mice. *Am J Physiol Endocrinol Metab* 2006;290(5):E814-E823.
25. Zhou D, Samovski D, Okunade AL, Stahl PD, Abumrad NA, Su X. CD36 level and trafficking are determinants of lipolysis in adipocytes. *FASEB J* 2012;26(11): 4733-4742.
26. Amer E, Westermark PO, Spalding KL, et al. Adipocyte turnover: relevance to human adipose tissue morphology. *Diabetes* 2010;59(1):105-109.
27. Weyer C, Foley JE, Bogardus C, Tataranni PA, Pratley RE. Enlarged subcutaneous abdominal adipocyte size, but not obesity itself, predicts type II diabetes independent of insulin resistance. *Diabetologia* 2000;43(12):1498-1506.
28. Lundgren M, Svensson M, Lindmark S, Renstrom F, Ruge T, Eriksson JW. Fat cell enlargement is an independent marker of insulin resistance and 'hyperleptinaemia'. *Diabetologia* 2007;50(3):625-633.
29. Kennedy DJ, Kuchibhotla S, Westfall KM, Silverstein RL, Morton RE, Febbraio M. A CD36-dependent pathway enhances macrophage and adipose tissue inflammation and impairs insulin signalling. *Cardiovasc Res* 2011;89(3):604-613.
30. Seppala-Lindroos A, Vehkavaara S, Hakkinen AM, et al. Fat accumulation in the liver is associated with defects in insulin suppression of glucose production and serum free fatty acids independent of obesity in normal men. *J Clin Endocrinol Metab* 2002;87(7):3023-3028.
31. Tiikkainen M, Tamminen M, Hakkinen AM, et al. Liver-fat accumulation and insulin resistance in obese women with previous gestational diabetes. *Obes Res* 2002; 10(9):859-867.
32. Coomans CP, Biermasz NR, Geerling JJ, et al. Stimulatory effect of insulin on glucose uptake by muscle involves the central nervous system in insulin-sensitive mice. *Diabetes* 2011;60(12):3132-3140.
33. Bays HE, Gonzalez-Campoy JM, Henry RR, et al. Is adiposopathy (sick fat) an endocrine disease? *Int J Clin Pract* 2008;62(10):1474-1483.